

A Stochastic Model of Human Gait Dynamics

Yosef Ashkenazy¹, Jeffrey M. Hausdorff², Plamen Ch. Ivanov^{1,2}, Ary L. Goldberger², and H. Eugene Stanley¹

¹ Center for Polymer Studies and Department of Physics, Boston University, Boston, Massachusetts 02215, USA

² Beth Israel Deaconess Medical Center, Harvard Medical School, Boston, Massachusetts 02215, USA

(April 29, 2024)

We present a stochastic model of gait rhythm dynamics, based on transitions between different “neural centers”, that reproduces distinctive statistical properties of normal human walking. By tuning one model parameter, the hopping range, the model can describe alterations in gait dynamics from childhood to adulthood — including a decrease in the correlation and volatility exponents with maturation. The model also generates time series with multifractal spectra whose broadness depends only on this parameter.

PACS numbers: 05.40.-a,87.15.Aa,87.90.+y

Many physical and physiological processes exhibit complex fluctuations characterized by scaling laws [1–8], some with monofractal [2] and others with multifractal behavior [3]. For example, normal gait dynamics of adults are monofractal [4], while healthy heartbeat fluctuations are multifractal [3]. The origin of these complex fluctuations and the factors that contribute to differences in their behavior are largely unknown. Here we develop a physiologically-motivated model that may be helpful in explaining some of the properties that contribute to complex dynamics. We focus on one class of signals — the time series of the inter-stride-intervals (ISI) between successive strides in human gait.

Walking is a voluntary process, but under normal circumstances, stride to stride regulation of gait is controlled by the nervous system in a largely automatic fashion [9,10]. Gait is regulated in part by “neural centers” within the cortex and the spinal cord [10]. As a result of time-varying inputs, neural activity at different times are thought to be dominated by different centers, leading to complex fluctuations in the ISI “output.” Furthermore, as the central nervous system matures from infancy to adulthood, the interaction between neural centers becomes richer [9].

To understand the underlying regulatory mechanisms of walking, deterministic and stochastic models have been proposed. For example, classic “central pattern generator” models are based on oscillatory neural activity, where the interaction between neural centers helps regulate gait dynamics [11]. A stochastic version of a central pattern generator model reproduces certain fractal properties of the ISI series [5]. However, existing models do not explain observed changes in scaling exponents [5], and volatility (magnitude) correlations [12,13] (a new finding reported in the present study) that occur during gait maturation from childhood to adulthood.

We propose a stochastic model consisting of a random walk (RW) on a chain, the elements of which represent excitable neural centers [14]. A step of the RW between element i and element j represents the “hopping” of the excitation from center i to center j . The increase of neu-

ral interconnectedness with maturation is modeled by increasing the range of “jump” sizes of the RW, since larger jump sizes will allow exploration of more neural centers. This property mimics one aspect of the increasing complexity of the adult nervous system.

Previous studies [15] have identified neural centers with pacemaker-like qualities that fire with frequency f_i , so we represent the network of neural centers by different frequency modes. One mode is activated at a given time ($ISI \propto 1/f_i$), and the f_i are Gaussian distributed. The model is based on the following assumptions (Fig. 1) :

- Assumption (i) is that the f_i have finite-size correlations, $\langle f_i f_{i+\delta} \rangle / \langle f_i^2 \rangle = e^{-\delta/\delta_0}$. We assume finite-range correlations among f_i because neighboring neurons are likely to be influenced by similar factors [10]. This assumption effectively creates “neuronal zones” composed of neural centers (modes) along the chain with a typical size δ_0 .
- Assumption (ii) concerns the rule followed by the RW process. The active neural center is determined by the location of the RW. The “jump” sizes of the RW follow a Gaussian distribution of width C .
- Assumption (iii) is that a small fraction of noise is added to the output of each mode to mimic biological noise not otherwise modeled. The output y becomes $y(1 + A\eta)$ where A is the noise level and η is Gaussian white noise with zero mean and unit variance [16].

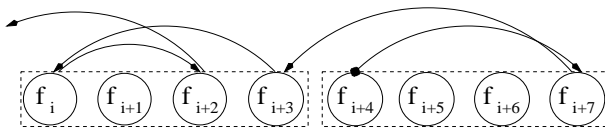


FIG. 1. Illustration of the “neural” hopping model. The values of f_i are not uncorrelated but rather have a finite size correlations. Shown is a sequence of four transitions, from mode f_{i+4} to f_{i+7} to f_{i+3} to f_i to f_{i+2} ... Larger values of the hopping-range parameter C are associated with larger “jump sizes” along the chain. The neuronal zone of size $\delta_0 = 4$ is indicated by the dashed boxes.

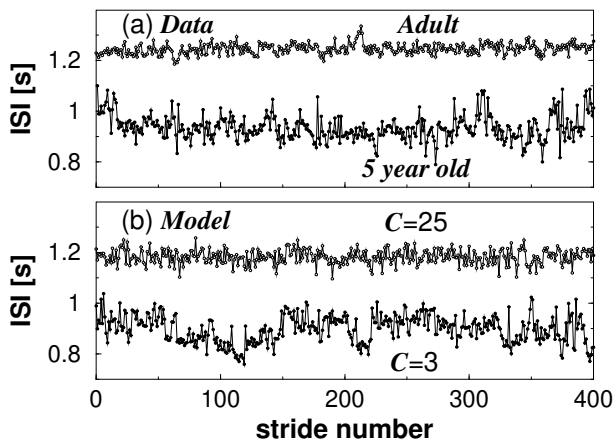


FIG. 2. (a) Examples of ISI series of healthy subjects, ages 5 and 25 years. (b) Examples of ISI generated by the model. Iterating the model with a small value of the hopping-range parameter ($C = 3$) mimics the ISI of young children, while a large value ($C = 25$) mimics that of adults.

The model has three parameters δ_0 , C , and A . We find that the best agreement with the data is achieved when $A = 0.02$ and $\delta_0 = 25$. In order to simulate changes with maturation, we vary only the third parameter, C , as a function of age, $C = (\text{age} - 2)$ for ages 3 to 25 years. Increasing the hopping range with age is consistent with the fact that neural transmission is not fully developed until the late teens [9,17].

Examples of ISI time series are shown in Fig. 2a. The ISI series of the adult subject has smaller fluctuations compared with the more variable ISI of the child. Two examples of the model’s output are shown in Fig. 2b; using a large value of C ($C = 25$) simulates the ISI series of an adult, while using a small value ($C = 3$) mimics the ISI series of a child. Surprisingly, we find that the normalized probability distributions of the child ISI increment series, $\Delta(\text{ISI})_i = (\text{ISI})_{i+1} - (\text{ISI})_i$, and of the model with small C are close to exponential (Fig. 3a). In contrast, the distribution converges to Gaussian in the adult and for large C in the model (Fig. 3b).

To further test the model, we study time correlations in the ISI series. We calculate the function $F(n)$, which corresponds to the rms fluctuations of the integrated ISI series of the adult (Fig. 2a) and of the model for $C = 25$ (Fig. 2b) [5,6,18]. Estimating the scaling exponent from the slope of $\log F(n)$ vs $\log n$, we find, for both data and model, that the ISI time series have correlations with scaling exponents ≈ 0.8 (Fig. 4a).

The scaling exponents of the original signal provide an indication of the linear properties (two-point correlations). Certain nonlinear aspects may be associated with the presence of long-range correlations in the magnitudes of ISI increments $|\Delta(\text{ISI})_i|$, an index of “volatility” [13]. We find (Fig. 4b) that the adult magnitude series is uncorrelated (the scaling exponent is close to 0.5). The model shows similar behavior for large C (Fig. 4b).

Next we inquire if changes in gait dynamics from childhood to adulthood might be reflected in changes in the scaling exponents of the ISI series. The short-range scaling exponents of the ISI series decrease as children mature [5]. We compare the short range scaling exponents for a group of 50 children [19] with those of 10 adults [5]; this exponent decreases from ~ 1.0 to ~ 0.7 (Fig. 5a). By altering C , the model simulates these maturation-related changes in two-point correlation properties.

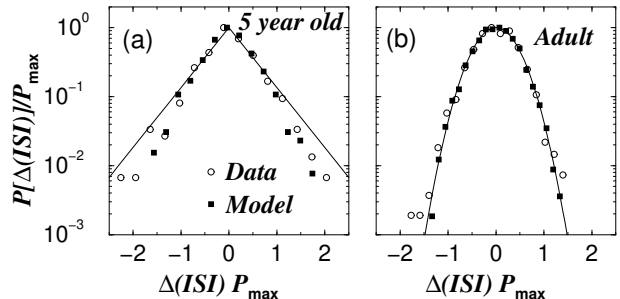


FIG. 3. (a) The normalized distribution of the increments of ISI series ($\Delta(\text{ISI})_i = (\text{ISI})_{i+1} - (\text{ISI})_i$) for the child’s ISI series (Fig. 2a) and for the model with $C = 3$ (Fig. 2b); both model and data are consistent with an exponential distribution, $P(x) = e^{-2|x|}$ (solid line). (b) Same as (a) for the adult shown in Fig. 2a and for model ($C = 25$) shown in Fig. 2b; in this histogram, both data and model are consistent with a Gaussian distribution, $P(x) = e^{-\pi x^2}$ (solid line).

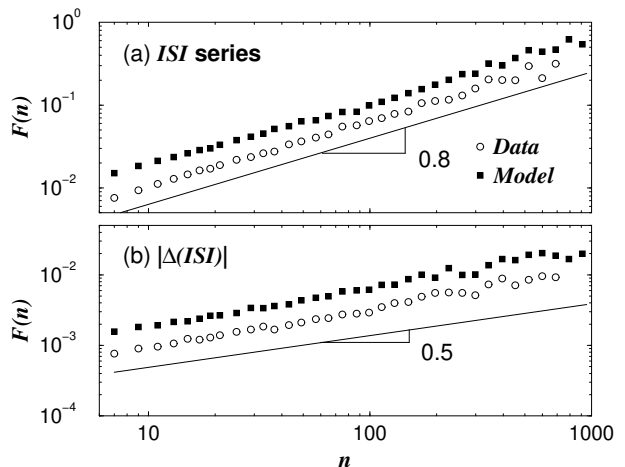


FIG. 4. (a) The rms fluctuation function $F(n)$ for the ISI series of adult (open circles) and of the simulation ($C = 25$, black squares) shown in Fig. 2. Here n indicates the window size in stride number. Both the data and the model have similar long-range correlation properties for the ISI series. (b) In contrast, $F(n)$ of the magnitudes of the ISI increments $|\Delta(\text{ISI})_i|$ shows weak correlations (scaling exponent of ≈ 0.55) where the scaling exponent of an uncorrelated series is ≈ 0.5 .

The magnitude series exponent of the ISI series also decreases with maturation (Fig. 5b). Our results for the

magnitude series suggest that the gait pattern of children is more volatile (and thus more nonlinear) than the

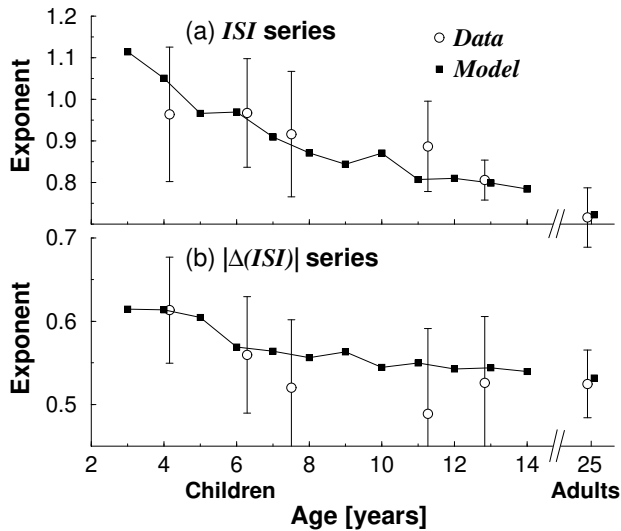


FIG. 5. The scaling exponents of the ISI series of the gait maturation database [19] and for the model. The gait maturation database consists of ISI time series from 50 children between 3 and 13 years old. Each time series is around 8 minutes (~ 500 data points). To study the effects of maturation, we divide the database into 5 subgroups: (i) 3-4 year olds (11 subjects), (ii) 5-6 year olds (10 subjects), (iii) 7-8 year olds (14 subjects), (iv) 10-11 year olds (10 subjects), and (v) 12-13 year olds (5 subjects). We also show data [5] from an adult group (10 subjects 1 hour long each; ages 20-30 years). Values for the scaling exponent axis are given as mean \pm standard deviation. For the model simulation, we generate 40 realizations for each value of C ; the average value is presented. The standard deviation around the average is ~ 0.06 for the original series and ~ 0.04 for the magnitude series. The age axis for the model follows the relation: age (years) = $C + 2$. (a) The short-range scaling exponents of the original time series both for the data (open circles) and the model (black squares). The exponents calculated for window sizes $6 < n < 13$ steps, decrease with age [5]. The scaling exponent obtained by the model decreases monotonically as C increases and is within the error bars of the data. (b) The scaling exponent of the ISI magnitude series, $|\Delta(ISI)_i|$. The magnitude scaling exponent is calculated for window size $6 < n < 64$ for the children’s group and $6 < n < 256$ for the adult’s group; the maximum window size is $\sim \frac{1}{10}$ of the series length for both groups. The magnitude scaling exponent decreases with age, indicating a loss of magnitude correlations with maturation. The model exhibits a similar decrease and the simulation is within the error bars of the actual data. The subject-to-subject variability is consistent with the scatter observed in physiologic indices of neural development [9].

usual walking pattern of adults. We note that: (i) unlike adults, young children have difficulty keeping their walking speed constant. A large “walking error” in one direction is likely to be followed by a large compensatory walking error in the opposite direction — i.e., a large (or

small) increment of ISI is likely to be followed by a large (or small) decrement over a given range of scales. This instability may lead to increased magnitude correlations. (ii) Adults can voluntarily simulate the less stable gait of children and thereby increase the magnitude correlations of the ISI. Children, however, cannot maintain the less volatile dynamics of adults. Thus, in general, the more mature adult gait dynamics are likely to be richer. The model shows (Fig. 5b) a similar decrease of the magnitude exponents when increasing C and is within the error bars of the data.

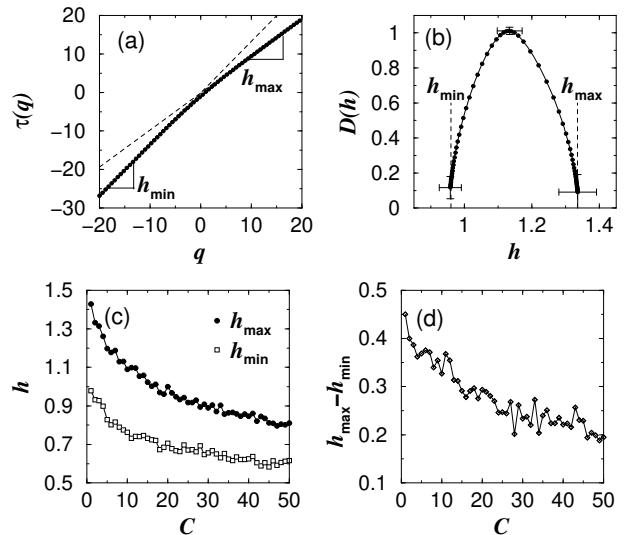


FIG. 6. The multifractal formalism applied to time series generated by the model. For the multifractal analysis, we applied the wavelet transform modulus maxima technique [20] with the Daubechies 10-tap discrete wavelet [21]. We integrate the series before applying the multifractal formalism. The parameters of the model are fixed (as described in the text) and only C changes. The series length is 32768 data points and for each value of C , we generate 10 realizations; the average value is presented. As the first step of the multifractal analysis we extract the partition function $Z_q(n)$ as a function of the window size n for different moments q . Then we estimate the scaling exponent $\tau(q)$ from the slope of $\log_2 Z_q(n)$ vs $\log_2 n$ where $4 \leq n \leq 2048$. (a) The exponent $\tau(q)$ vs the moment q for $C = 2$. (b) The Legendre transform $D(h) = qh - \tau(q)$ of (a) where $h(q) = d\tau/dq$ and $D(h)$ is the multifractal spectrum. The maximum and minimum Holder exponents, h_{\max} and h_{\min} are indicated by dashed lines and estimated as the slope of $\tau(q)$ for $-20 < q \leq -15$ and $15 \leq q < 20$, respectively (see the dashed lines in (a)). Error bars (1 standard deviation) are shown for both axes for $q = -20$, $q = 0$, and $q = 20$. (c) h_{\max} and h_{\min} for different values of C . A smaller C value yields a broader multifractal spectrum. The error bars are as indicated in (b). (d) The broadness of the multifractal spectrum, $h_{\max} - h_{\min}$, as a function of C . For larger C , the multifractal spectrum becomes narrower. For $C \gg 1$ $h_{\max} \sim h_{\min} \sim 0.5$.

The decrease of the magnitude exponent with maturation is consistent with the possibility that the ISI time

series (during goal-directed walking) becomes less multifractal as the individual matures. This prediction cannot be tested on the available data since the time series of the children are too short for multifractal analysis; but this prediction can be tested on the model. Fig. 6 summarizes a systematic multifractal analysis on ISI series generated by the model. We find narrower multifractal spectra with increasing C , suggesting the possibility of a decrease of multifractality with maturation during normal walking. The model's prediction agrees with a recent finding regarding the monofractality of normal gait in adults [4]. The model also serves as a generator of random series with different multifractal spectra — multifractal for $C \approx 1$ and monofractal for $C \gg 1$.

In summary, we find that a simple stochastic model captures multiple aspects of gait dynamics, and their changes with maturation, including: (i) the shape of the probability distribution of the ISI increments; (ii) correlation properties of the ISI; and (iii) correlations properties in the magnitudes of the ISI increments [22]. Further, by varying only a single “hopping-range” parameter, C , a wide array of multifractal dynamics can be generated. The model can also be altered by “knocking out” certain frequency modes (akin to what may occur during very advanced age or in response to neurodegenerative disease). Simulation with drop-out of frequency modes predicts increased gait variability, with (i) increased magnitude exponents, and (ii) decrease of long-range correlations. Our preliminary analysis of the ISI series of older adults prone to falls is consistent with this prediction. Generalization of the model to two and three dimensional networks to describe other types of neurological activities is underway.

Partial support was provided by the NIH/National Center for Research Resources (P41 RR13622) and the NIA (AG14100). We thank J.J. Collins, S. Havlin, V. Schulte-Frohlinde, and C.-K Peng for helpful discussions.

[1] M.F. Shlesinger, Ann. NY Acad. Sci. **504**, 214 (1987).
 [2] A. Arneodo *et al.*, Phys. Rev. Lett. **74**, 3293 (1995).
 [3] P.Ch. Ivanov *et al.*, Nature **399**, 461 (1999).
 [4] P.Ch. Ivanov *et al.* (unpublished).
 [5] J.M. Hausdorff *et al.*, J. Appl. Physiol. **78**, 349 (1995); *ibid.* **80**, 1448 (1996); *ibid.* **82**, 262 (1997); *ibid.* **86**, 1040 (1999).
 [6] B.J. West and L. Griffin, Fractals **6**, 101 (1998).
 [7] J.J. Collins and C.J. De Luca, Phys. Rev. Lett. **73**, 764 (1994).
 [8] Y. Chen *et al.*, Phys. Rev. Lett. **79**, 4501 (1997).
 [9] Central nervous system myelination is not fully complete until the late teens. Consequently, neural processing and the speed of neural transmission do not reach maximum

values until this point, consistent with increasing neural interactions with maturation. See J.M. Schroder *et al.*, Acta Neuropathol. **76**, 471 (1988); A. Pfefferbaum *et al.*, Arch. Neurol. **51**, 874 (1994).
 [10] J.M. Winters and P.E. Crago (eds.), *Biomechanics and Neural Control of Posture and Movement* (Springer-Verlag, New York, 2000).
 [11] J.H. McAuley and C.D. Marsden, Brain **123**, 1545 (2000); J.J. Collins and I. Stewart, Biol. Cybern. **68**, 287 (1993); M. Golubitsky *et al.*, Nature **401**, 693 (1999); G. Taga *et al.*, Biol. Cybern. **65**, 147 (1991).
 [12] Y. Liu *et al.*, Phys. Rev. E **60**, 1390 (1999).
 [13] Other studies define volatility as the local variance of the signal. Here by volatility correlations we mean correlation in the magnitudes of the series increments. Y. Ashkenazy *et al.*, Phys. Rev. Lett. **86**, 1900 (2001).
 [14] We model one specific type of human locomotion, namely “usual” or “directed” gait. This type of voluntary, goal-directed activity has a large automatic component and usually tends to minimize variability. Other types of locomotor activity (not modeled here) would include more “free-form” patterns of gait, as well as recreational movements during dance or sports.
 [15] D. Plenz and S.T. Kital, Nature **400**, 677 (1999).
 [16] It is possible to add the following assumption in order to capture the observed decrease of ISI variability with age as children mature [5]. When in a mode of frequency f_i , the model generates as an output $ISI = B/f_i$. We suggest the proportionality constant, B , to be the ratio between the number of simulated strides and the number of active modes (i.e., the number of different modes that were visited during a simulation). Then, the standard deviation of the output of the model decreases when C increases with no effect on the model dynamics.
 [17] The model's dynamics can be understood in the following intuitive way. For $C \ll \delta_0$ (small hopping-range, young child), the dynamics will be confined mainly to a single “neuronal zone”; this will lead to correlations in the ISI time series. For $C \approx \delta_0$ (large hopping-range, adult) the dynamics will explore frequency modes from different zones; this will lead to a decrease in the correlations. Moreover, for $C \ll \delta_0$ the dynamics changes back and forth from one mode to a nearby mode leading to increased magnitude correlations. For $C \approx \delta_0$ the dynamics are governed by many different modes leading to the loss of magnitude correlations.
 [18] We use detrended fluctuation analysis for the scaling analysis: C.-K. Peng *et al.*, Phys. Rev. E **49**, 1685 (1994).
 [19] <http://www.physionet.org/> (Gait Maturation Database); see also A.L. Goldberger *et al.*, Circulation **101**, e215 (2000).
 [20] J.F. Muzy, *et al.*, Phys. Rev. Lett. **67**, 3515 (1991); A. Arneodo *et al.*, J. Math. Phys. **39**, 4142 (1998).
 [21] Daubechies I., *Ten Lectures on Wavelets* (S.I.A.M., Philadelphia, PA, 1992).
 [22] While there is good agreement between the model output and the data for these orthogonal dynamical properties, both in adults and as a function of maturation, further study is required to investigate the physiologic analogs that generate these dynamical properties.